MHD performance limits in JET Optimised Shear Discharges

P. Hennequin[1], T.C Hender[2], B. Alper[2], C.D Challis[2], N.C Hawkes[2], T. Hellsten[4], D.F. Howell[2], G.T.A Huysmans[3], X. Litaudon[3], P. Lotte[3], P. Maget[3], J. Manickam[5], M. Maraschek[6], D. Mazon[3], M. F Nave[7], A. Pochelon[8], S. Sharapov[2], and contributors to the EFDA-JET workprogramme [1]

[1] *LPTP, CNRS UMR7648, Ecole Polytechnique, 91128 Palaiseau, France*
[2] *Euratom-UKAEA Fusion Assoc, Culham Science Centre, Abingdon, UK*
[3] *Association Euratom-CEA, DRFC, Cadarache, 13 108 St Paul lez Durance, France*
[4] *EFDA-JET, Abingdon, Oxfordshire, OX14 3EA, UK*
[5] *PPPL, Princeton, N.J. 08543, USA*
[6] *IPP/Euratom Association, Boltzmannstr. 2 D-85478 Garching Germany*
[7] *Associaçiao Euratom/IST, Centro de Fusao Nuclear, 1096 Lisbon, Portugal*
[8] *CRPP/EPFL, Association Euratom-Confédération Suisse, 1015 Lausanne, Switzerland*

Introduction

Optimised Shear discharges, producing Internal Transport Barriers (ITB), are considered as attractive reactor-relevant scenarios, since they combine high confinement, high bootstrap current, and high normalised beta. ITBs are obtained on JET, by applying the main heating (ICRH, NBI) during current ramp-up, after an LHCD pre-heat phase, leading to negative central magnetic shear [1]. Due to the steep pressure gradients achieved at the internal transport barrier and to the shape of the safety factor profile, MHD activity affects these high performance steady-state scenarios, by degrading the improved confinement or even leading to disruptions.

In the set of high performance JET discharges considered here, LHCD was used in the pre-heat phase in order to control the current profile evolution allowing strongly non-monotonic q-profiles to be obtained [1, 2, 3]. In such scenarios the main limitations to high performance, i.e. the neutron rate, experimentally observed are disruptions and large, long lived $n = 1$ modes. The latter have sometimes shown a double tearing structure. Other MHD phenomena can to varying degrees affect the ITB performance, especially $n = 1$ bursts associated with a rapid drop of the pressure profile (collapses that can be observed during the main heating phase, in addition to the high q sawtoothing behaviour generally occurring during the LHCD prelude phase, [4, 5, 6]). The performance generally recovers after these short events, unless an ELM free phase occurs followed by large ELMs which lead to an irreversible loss of the ITB.

This $n = 1$ activity is a new feature of the negative magnetic shear scenarios. Conversely, $q = 2$ snakes and medium n tearing modes, characteristic of the OS discharges with monotonic profiles and weak central shear [7], were scarcely observed. R_{nt} rollover may also occur without associated MHD, caused either by interaction with the septum, impurity radiation or transport bifurcation, or transition to Elm free period or type I Elms.

I. MHD terminating the ITB: Disruptions

The most common limitation to the performance in OS discharges are disruptions affecting around 1/3 of the pulses with a neutron rate $R_{nt} > 1.6\,10^{16} s-1$ at rollover. The ideal kink mode driven by the steep pressure gradient at the ITB is commonly found to be responsible for these disruptions, similarly to the observations on JET with low central magnetic shear scenarios [8], and on other tokamaks [10, 11].

[1]See annex of J. Pamela et al, "Overview of Recent JET Results and Future Perspectives", Fusion Energy 2000 (Proc. 18th Int. Conf. Sorrento, 2000), IAEA, Vienna (2001).

The normalized beta β_N at the disruption is typically between 1 and up to 2.5, depending on the peaking factor of the pressure profile.

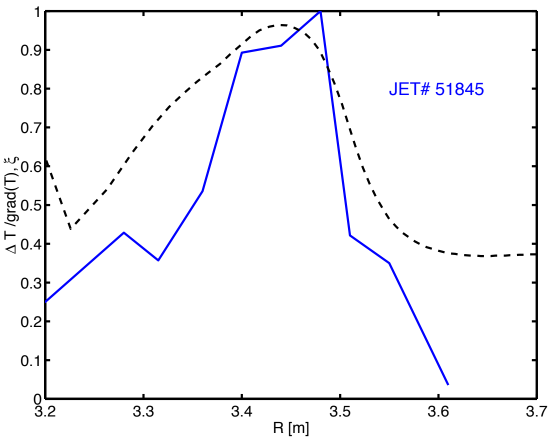

Fig 1: Displacement along the horizontal axis just before the disruption, inferred from ECE measurements (plain), shot #51845, compared with the envelop of the unstable calculated eigenfunction (dashed).

Some disruptions have very clear $n = 1$ precursors which have a global structure without phase inversions (ideal mode).
Stability analyses have been performed with the MISHKA [8] and PEST [12] codes, based on the linear MHD model.
The observed mode structures are in good agreement with the calculated mode structures for the $n = 1$ ideal pressure driven kink mode, as shown in figure 1. The calculated eigenfunction is obtained from a PEST run using equilibria from TRANSP (shot #51845), and shows the global structure of the mode. The calculated β at the disruption is also quite consistent with the calculated limits (1.5% for the case shown).

Simulations show small differences in the mode structure of the disruptions between reversed shear and low shear discharges (larger $m = 1$ component in RS case). In both cases, the observed mode vanishes more rapidly than the calculated one at the edge.

Accessing higher β limits for the pressure driven kink mode can be achieved by changing the shape of the pressure profile, by varying the time of the heating (and target q profile) or controlling the heating power, allowing the barrier to expand outwards.

II. MHD terminating ITB: Large $n = 1$ modes

Large performance reduction is also observed due to the onset of large $n = 1$ modes during the ITB (1/3 of the discharges considered), as can be seen on figure 2. The ITB starts slightly before 9s, and the drop of the neutron rate (trace b) coincides with the onset of MHD activity (trace d) at 9.25s.

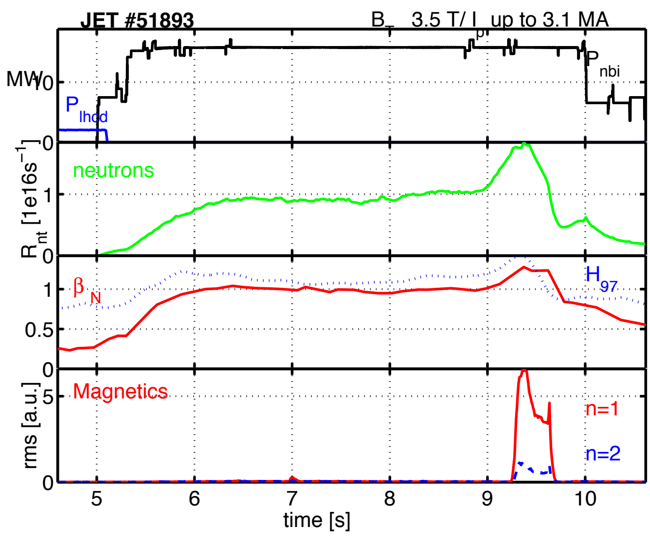

Fig. 2: Time history for shot # 51893 : (a) applied power ; (b) the neutron rate; (c) normalised beta β_N and performance factor H97; (d) rms value of the magnetic probe signal

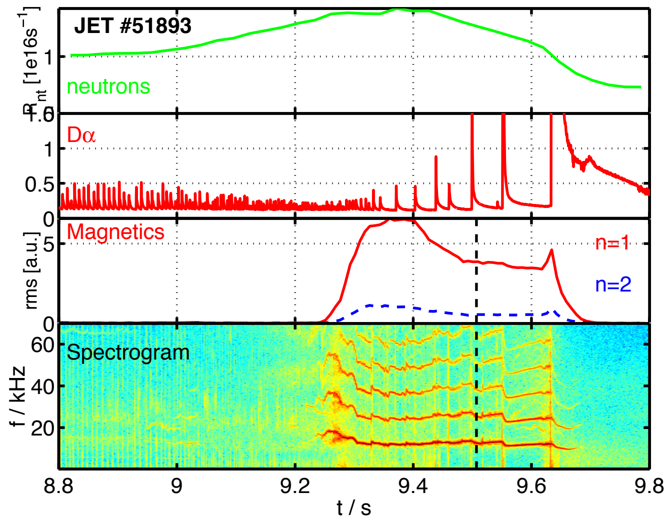

The spectrogram of magnetic probe signals (figure 3,d) shows a typical multi-harmonic signature.
These large modes erode the barrier inwards, increasing the edge temperature until a large ELM kills the barrier completely (the transition in the Elms activity (type III to I) is also shown in figure 3 (b)).

Fig. 3: detail of the rollover ((c) rms amplitude (d) spectrogram of pick-up coil signals).

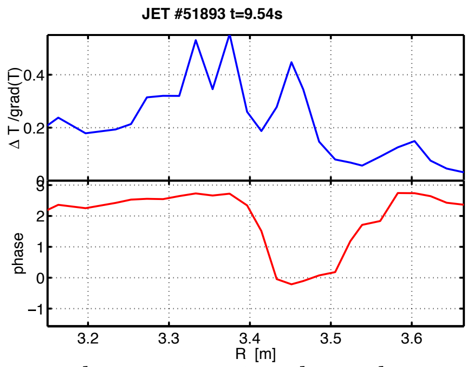

A fast acquisition of magnetic and temperature data at 9.5s allows analysis of the detailed structure of the mode. The lowest harmonic, with a toroidal mode number value of 1, has a double tearing mode structure (fig.4)

Fig. 4: amplitude and phase of the ECE signal fourier components (f $\sim$ 13kHz), shot #51893. The double phase shift indicates a double tearing mode.

Note that the fast data are not recorded here at the mode starting time but when it is well developed. Unfortunatly the very limited number of shots with fast data during the large $n = 1$ mode makes it impossible to draw general conclusions on their nature. They could be ideal modes then evolving to resistive nature, as seen in Asdex [10].

These modes are different to the snakes previously observed in weak shear OS discharges, which also presented a multi-harmonic spectrum, but were much more localised both radially (at the foot of the barrier), and poloidally.

III. Long lived tearing modes throughout main heating phase.

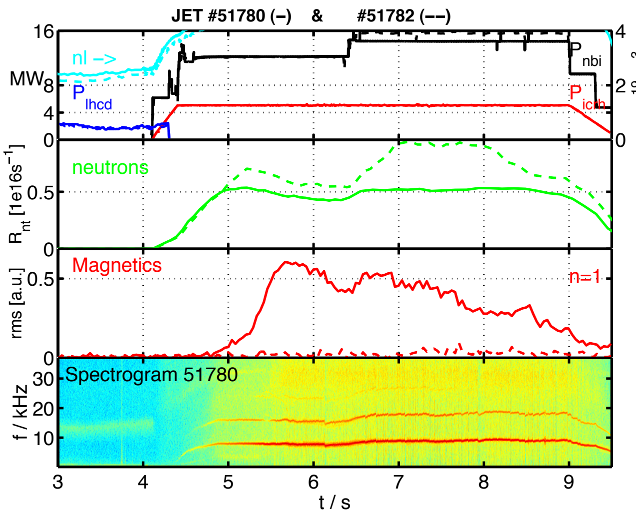

In addition to possibly terminating the high performance phase, double tearing modes also sometimes prevent the ITB formation. This is the case for shot #51780 shown in Figure 5 (plain). The mode structure was confirmed using fast magnetics and ECE data. By comparison, shot #51782 achieves ITB formation with a high β_p [3], by slightly varying the target q-profile (same power waveform but lower density in the pre-heat phase [4]).

Fig. 5: shots #51780 (plain) and #51782 (dashed). Spectrogram of shot #51780.

IV. Bursts of $n = 1$ activity.

Short lived activity can also temporarily cause temperature rollover. These bursts are associated with sawteeth-like collapses [5, 6] occurring during the main heating phase

(ECE temperature time traces, figure 6 (b)). The ITB generally recovers after the smaller events, but transition to type I Elm sometimes occurs due to erosion of the barrier.

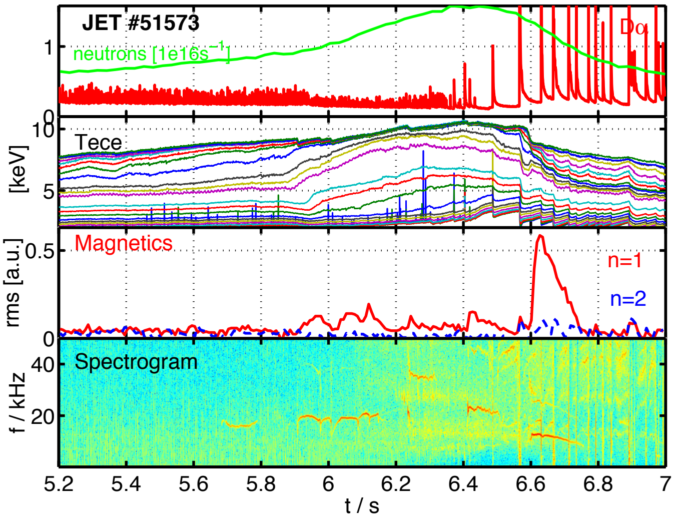

Fig. 6:Time history of shot #51573 .

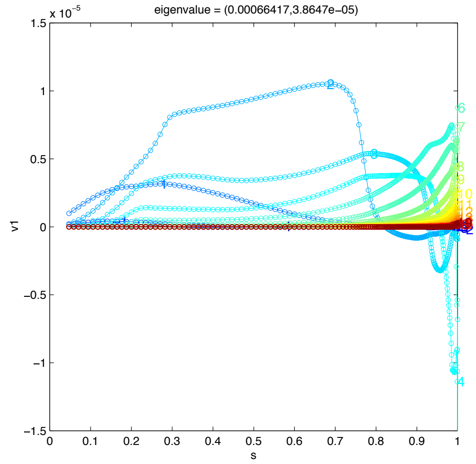

Fig. 7: poloidal harmonics of the calculated displacement vs normalised radius, shot #51573, MISHKA .

The largest bursts have been mostly identified as ideal modes located between rational q surfaces ($q = 2$ or 3, depending on q_{min}), with the same structure as the mode observed before a disruption (§ **I.**). This is similar to previous observations in weak shear discharges [8]. The difference between cases which lead to a disruption and benign ones is still unclear but maybe related to the more localized mode structure in the case of negative central shear with two q=2 surfaces. The structure of the mode calculated with MISHKA (fig. 7), using pressure and safety factor profiles from TRANSP, agrees with these observations, as well as the calculated β limit (experimental $\beta_p \sim 0.83$).

Smaller bursts are located in the negative shear zone of the q profile (extend $\sim$ 10 cm at a low order rational q), mainly affecting the inner part of the barrier. They have been analysed with the CASTOR code, using the same profiles : $n = 1$ resistive interchange modes are found to be unstable and agreement with observations seems to be good, especially the localisation.

Summary.

MHD phenomena can affect to varying degrees the ITB performance. The most severe is the disruption limit. In many cases disruptions have a $n = 1$ pre-cursor and are due to ideal pressure driven kink modes. Bursts of $n = 1$ modes, which have the same ideal structure of modes preceding the disruption, temporarily affects the performance. Finally large $n = 1$ (tearing) modes can terminate the ITB phase, or prevent its formation.

[1] C. Challis , *et al.*. *This Conference (28th EPS),* P2.008.
[2]N.C. Hawkes, *et al.*, *This Conference (28th EPS),* Or02, P2.021.
[3] X. Litaudon , *et al.*, *This Conference (28th EPS)*, Or22.
[4] J. Mailloux, *et al.*, *This Conference (28th EPS)*, P2.084.
[5] D. Hogeweij, *et al.*, *This Conference (28th EPS)*, P2.002.
[6] T. Hellsten, *et al.*, *This Conference (28th EPS)*, P2.024.
[7] T.C. Hender, *et al.*, in *Proc. of 26th EPS PPCF Conf.*, Maastricht, June 1999. Or23.
[8] G.T. Huysmans, *et al.*. *Nuclear Fusion*, **39** ,1489, (1999).
[9] S. Gunter, *et al.*. *Nuclear Fusion*, **40**,1541 (2000).
[10] M. Okabayashi, E. Fredrickson, J. Manickam, *et al.*. *Nuclear Fusion*, **38**, 1149 (1998)
[11] R. C. Grimm, R. L. Dewar, and J. Manickam. *J. Comput. Phys.* **49**, 94 (1983)

This work has been conducted under the European Fusion Development Agreement, and was partly funded by Euratom (contrat CEA V.2939.0003).